THE ENDOCRINE SOCIETY MOLECULAR ENDOCRINOLOGY
About MEND Submission Subscription

Mol Endocrinol. 2013 Dec; 27(12): 2116–2125.
Published online 2013 Nov 6.
doi: 10.1210/me.2013-1146: 10.1210/me.2013-1146

PMCID: PMC3857197
PMID: 24196349

VDR Attenuates Acute Lung Injury by Blocking Ang-2-Tie-2 Pathway and Renin-Angiotensin System

Juan Kong,* Xiangdong Zhu, Yongyan Shi, Tianjing Liu, Yunzi Chen, Ishir Bhan, Qun Zhao, Ravi Thadhani,* and Yan Chun Li*

Department of Medicine (J.K., X.Z., Y.S., T.L., Y.C., Y.C.L.), Division of Biological Sciences, The University of Chicago, Chicago, Illinois 60637; Laboratory of Metabolic Disease Research and Drug Development and (J.K., Y.C., Y.C.L.), Department of Pediatrics (Y.S.), and Ministry of Health Key Laboratory of Congenital Malformation (T.L., Q.Z.), Shengjing Hospital, China Medical University, Shenyang, 110000, China; and Division of Nephrology (I.B., R.T.), Massachusetts General Hospital, Harvard Medical School, Boston, Massachusetts 02114

*Corresponding author.

Address all correspondence and requests for reprints to: Juan Kong, Laboratory of Metabolic Disease Research and Drug Development and Shengjing Hospital, China Medical University, Shenyang, 110000, China;, E-mail: kong_juan@hotmail.com; Ravi Thadhani, M.D., M.P.H., Renal Unit, Massachusetts General Hospital, Harvard Medical School, Boston, Massachusetts 02114., E-mail: thadhani.ravi@mgh.harvard.edu; and Yan Chun Li, Ph.D., Department of Medicine, The University of Chicago, 900 East 57th Street, KCBD 9110, Chicago, Illinois 60637., E-mail: cyan@medicine.bsd.uchicago.edu.

Received 2013 May 17; Accepted 2013 Oct 23.

Abstract

Acute lung injury (ALI) is a hallmark of systemic inflammation associated with high mortality. Although the vitamin D receptor (VDR) is highly expressed in the lung, its role in lung physiology remains unclear. We investigated the effect of VDR deletion on ALI using a lipopolysaccharide (LPS)-induced sepsis model. After LPS challenge VDR-null mice exhibited more severe ALI and higher mortality compared with wild-type (WT) counterparts, manifested by increased pulmonary vascular leakiness, pulmonary edema, apoptosis, neutrophil infiltration, and pulmonary inflammation, which was accompanied by excessive induction of angiopoietin (Ang)-2 and myosin light chain (MLC) phosphorylation in the lung. 1,25-Dihydroxyvitamin D blocked LPS-induced Ang-2 expression by blocking nuclear factor-κB activation in human pulmonary artery endothelial cells. The severity of lung injury seen in VDR-null mice was ameliorated by pretreatment with L1–10, an antagonist of Ang-2, suggesting that VDR signaling protects the pulmonary vascular barrier by targeting the Ang-2-Tie-2-MLC kinase cascade. Severe ALI in

VDR-null mice was also accompanied by an increase in pulmonary renin and angiotensin II levels, and pretreatment of VDR-null mice with angiotensin II type 1 receptor blocker losartan partially ameliorated the severity of LPS-induced lung injury. Taken together, these observations provide evidence that the vitamin D-VDR signaling prevents lung injury by blocking the Ang-2-Tie-2-MLC kinase cascade and the renin-angiotensin system.

The lung has 2 anatomic compartments: the airway compartment and the vascular compartment. Alveolar epithelial cells line the airway compartment, and pulmonary endothelial cells line the vascular compartment. These cells are vital for maintaining the integrity of the air-blood barrier (1). The endothelial cells form a semipermeable barrier between the blood and the interstitium of the lung. This endothelial barrier is tightly regulated. Increased vascular permeability is a hallmark of acute lung injury (ALI) and acute respiratory distress syndrome (ARDS), major pulmonary complications of systemic inflammation that carry a high risk of mortality. Disruption of the endothelial barrier results in paracellular movement of fluid and macromolecules (including blood cells) from the blood to the interstitium and pulmonary air space. The development of pulmonary edema impairs gas exchange and precipitates respiratory failure (2).

The paracellular space of the endothelial barrier is sealed by intercellular junctions including tight junctions and adherens junctions. A body of evidence has demonstrated that phosphorylation of myosin light chains (MLCs) is one of the key regulatory steps controlling vascular permeability (3–5). Activation of MLC kinase (MLCK) phosphorylates MLCs, leading to increased endothelial contractile force and thus increased vascular permeability (6).

Endotoxin lipopolysacchride (LPS)-induced activation of the angiopoietin (Ang)-2-Tie-2 signaling pathway plays a crucial role in the development of sepsis-associated ALI and ARDS. Ang-1 and Ang-2 are peptide ligands that bind to Tie-2 receptor tyrosine kinase found primarily in endothelial cells. Tie-2 is highly expressed in the lung (7), and disruption of the Tie-2 signaling pathway leads to developmental lung disorders (8). Ang-1 has activity to inhibit inflammation and maintain vascular permeability (9), and overexpression of Ang-1 in mesenchymal stem cells prevents LPS-induced ALI in mice (10). In contrast, Ang-2 increases vascular permeability and promotes ALI. Excess circulating Ang-2 has been linked to pulmonary vascular leak in humans with sepsis (11, 12). Ang-2 is produced primarily by endothelial cells (13), thus affecting endothelial cells in an autocrine or paracrine fashion. In fact, LPS induces Ang-2 while suppressing Ang-1 in endothelial cells (14). LPS also induces lung inflammation and vascular leakage via activation of MLCK (15). Ang-2 can disrupt endothelial barrier via phosphorylating MLCs (11), indicating a critical role of Ang-2-Tie-2-MLCK cascade in LPS-induced vascular injury and ALI.

Emerging evidence also suggests that the renin-angiotensin system (RAS) plays a role in LPS-induced ALI. LPS increases angiotensin-converting enzyme in the lung, and high levels of circulating angiotensin II have been found in patients with ARDS (16). Systemic infusion of angiotensin II promotes ALI, and pharmacologic blockade of the RAS cascade ameliorates LPS-induced ALI in animals (17, 18).

The vitamin D receptor (VDR) is a member of the nuclear receptor superfamily (19, 20) that mediates the activities of 1,25-dihydroxyvitamin D [$1,25(OH)_2D_3$], the hormonal form of vitamin D. Recent studies have established that $1,25(OH)_2D_3$ is a pleiotropic hormone with broad biological activities that extend beyond the regulation of calcium and phosphate homeostasis (21). Tissues that express a high level of

VDR include the gastrointestinal tract, kidney, skin, immune system, and lung. A great deal of knowledge has been obtained in the past decade with regard to VDR's functions in these tissues, with a notable exception for the lung. Published studies that concern vitamin D/VDR and the respiratory system are largely limited to studies of asthma (22–24). Generally speaking, the biologic function of the VDR in the lung remains to be defined. In this study we investigated the effect of VDR deletion on LPS-induced ALI in mice. Our data suggest that VDR-mediated $1,25(OH)_2D_3$ actions protect against sepsis-induced lung injury by inhibiting the Ang-2-Tie-2-MLCK pathway as well as the RAS cascade.

Materials and Methods

Animals and treatment

The animal study protocols were approved by the Institutional Animal Care and Use Committee at The University of Chicago. VDR-null (knockout [KO]) mice in C57BL/6 and CD1 backgrounds were described previously (25). To prevent hypocalcemia, VDR-null mice were weaned on a high-calcium diet (Harlan Teklad TD96348: 20% lactose, 2% calcium, and 1.25% phosphorus) as reported previously (26). To induce lung injury, 2- to 3-month-old VDR KO and wild-type (WT) mice were injected ip with one dose (20 mg/kg) of lipopolysaccharide (LPS, O111:B4, Sigma L2630). Experimental groups were balanced in both sexes. After 24 hours, broncho-alveolar lavage (BAL) was collected, and the lung was harvested to assess injury. Blood was also collected for plasma cytokine assays. In some experiments, mice were pretreated by sc injection of L1–10 (provided by Amgen) at 2 mg/kg/d, 3 times/wk for 2 weeks or by feeding water containing 0.25 mg/mL of losartan for 2 weeks before being challenged with LPS.

Assessment of lung injury

Lung injury was assessed using several methods. 1) Evans blue permeability assay: Evans blue (2%, MP Biomedicals) was delivered by retro-orbital injection 10 minutes before killing the mice. This assay was used to measure pulmonary vascular leakiness caused by endothelial barrier damage. The content of Evans blue leaked into the lung intestitium was extracted and quantified by spectrophotometer (620 nm and 740 nm) as described previously (27); 2) Pulmonary fluid retention was assessed by subtracting the dry weight from the wet weight of the lung normalized to body weight as described elsewhere (28); 3) Measurement of protein concentration and cell number in the BAL fluid. These data represent protein leak and cell infiltration from the circulation into the broncho-alveolar space in the lung; 4) Measurement of myeloperoxidase (MPO) activity. MPO is a neutrophil-specific enzyme and serves as an inflammatory marker; thus MPO activity accounts for neutrophil infiltration into the lung. The activity was assayed in lung lysates or BAL fluid using a commercial MPO assay kit (CytoStore) according to manufacturer's instruction; and 5) Respiratory elastic resistance was measured using a computer-controlled ventilator (Flexivent, SCIREQ) as described elsewhere (29). This was a direct assessment of lung function (respiratory mechanics).

Measurement of cytokines

TNFα and IL-6 concentrations in the serum or BAL were determined by ELISA using commercial kits obtained from BioLegend.

Angiotensin II assays

Angiotensin II concentration in the BAL fluid was determined using a Human/Mouse/Rat Angiotensin II Enzyme Immunoassay Kit (Ray Biotech, Inc) according to manufacturer's instructions.

Renin activity assays

Renin activity in BAL fluid was determined using a Fluorimetric Sensolyte 520 Mouse Renin Assay Kit (AnaSpec, Inc) following the manufacturer's protocol.

Histology, immunostaining, and terminal deoxynucleotide transferase-mediated dUTP nick end labeling (TUNEL) staining

The lung was fixed in 10% formalin, processed and sectioned at 3 μm using a Leica microtome. Sections were examined by routine hematoxylin and eosin staining. Sections were also stained with fluorescein isothiocyanate-conjugated neutrophil-specific monoclonal antibody 7/4 (ab53453, Abcam) to assess neutrophil infiltration. Lung cell apoptosis was assessed by TUNEL staining, using ApopTag Plus Peroxidase In Situ Apoptosis Detection Kit (Chemicon) according to the manufacturer's instruction as described previously (30). Apoptosis was semiquantified by assessing TUNEL-positive microscopic fields in randomly chosen 50 fields in each mouse, and apoptotic index was defined as percentage of TUNEL-positive cell-containing fields.

Human pulmonary artery (PA) endothelial (HPAE) cell culture

HPAE cells were cultured in Clonetics EBM-2 media (CC-3156, Lonza) supplemented with EGM-2 BulletKit (Lonza), 10% fetal bovine serum, 100 U/mL penicillin, 100 mg/mL streptomycin according to the manufacturer's instructions. The cells were usually treated with 100 ng/mL LPS for 0–36 hours with or without overnight pretreatment with 20 nM $1,25(OH)_2D_3$, followed by isolation of total RNAs, total cell lysates, or nuclear extracts for various assays.

RT-PCR

Total RNAs were extracted using TRIzol reagent (Invitrogen). First-strand cDNAs were synthesized from total RNAs using MML-V reverse transcriptase (Invitrogen) and hexanucleotide random primers. Regular RT-PCR was performed using a DNA Engine (Bio-Rad Laboratories). Real-time RT-PCR was carried out in a 7900 Real Time PCR System using a SYBR green PCR reagent kit (Applied Biosystems) as described previously (31). PCR primers used in the study are: mAng-2-forward (F), 5′-GATCTTCCTCCAGCCCCTAC-3′ and mAng-2-reverse (R), 5′-GGGCTTCCACATCAGTCAGT-3′; hANG-2-F, 5′-TCTAAGGACCCCACTGTTGC-3′, and hANG-2-R, 5′-CCCAGCCAATATTCTCCTGA-3′; hVDR-F, 5′-CGTGTGAATGATGGTGGAGGGAGCC-3′, and hVDR-R, 5′-GTCTTGGTTGCCACAGGTCCAG-3′. β-2 Microglobulin served as an internal control.

Western blot

Total lung lysates were prepared by homogenizing lung tissues in Laemmli buffer. Total BAL proteins were precipitated with acetone and dissolved in Laemmli buffer. Proteins were separated by SDS-PAGE and electroblotted onto Immobilon-P membranes. Western blotting analyses were carried out as previously

described (32). The antibodies used in this study included: MLC (catalog no. 8505) and phospho-MLC (catalog no. 3674) from Cell Signaling Technology; and angiopoitin-2 (C19) (sc-7051), Tie-2 (C20) (sc-324), and MLCK(L-18) (sc-9452) from Santa Cruz Biotechnology. Secondary antibody was horseradish peroxidase-conjugated antirabbit IgG (Pierce Biotechnology), and signals were detected using SuperSignal West Dura Extended Duration Substrate (Pierce). The relative amount of proteins was quantified using gel analysis software UNSCAN-IT gel version 5.3 (Silk Scientific) and normalized to β-actin internal loading control.

EMSA

EMSA was used to validate the functionality of the κB binding site within the first intron of human *Ang-2* gene. EMSA was performed using ^{32}P-labeled ANG-2 κB double-stranded probe 5′-CCCCT*GGGCATTTCC*TAGGC3-′ (underlined is κB site) and nuclear extracts of HPAE cells as described elsewhere (33).

Chromatin immunoprecipitation (ChIP) assays

HPAE cells pretreated with or without 20 nM 1,25(OH)$_2$D$_3$ for 24 hours were stimulated with LPS for 2 hours. ChIP assays were performed as described previously (33), using anti-p65 antibodies. PCR was carried out using primers flanking the κB site (5′-GGGCATTTCC-3′) within the first intron of human *ANG-2* gene: Ang-2-PCR1, 5′-CAGCTTAGCACGGCAAAAAT-3′ and Ang-2-PCR2, 5′-TGGCAACAGGAAAAATCAGA-3′.

Statistical analysis

Data values were presented as means ± SD. Statistical comparisons were carried out using unpaired 2-tailed Student's *t* test or ANOVA as appropriate, with $P < .05$ being considered statistically significant.

Results

VDR inactivation increases the severity of lung injury following LPS challenge

We first explored the effect of VDR inactivation on lung injury using mouse sepsis model, because ALI is a major cause of death in sepsis. When WT and VDR KO mice (Figure 1A) were treated by a lethal dose (LD) of LPS (via ip injection), VDR KO mice showed much higher mortality. By 72 hours all VDR KO mice died, whereas 60% of WT mice remained alive at 96 hours (Figure 1B). Histologic examination showed no obvious difference in the lung structure between WT and VDR KO mice at baseline (Figure 1 C). After LPS administration there was a marked increase in alveolar wall thickness in both genotypes; however, the thickening of the alveolar interstitial space was demonstrably more robust in KO mice (Figure 1C), suggesting more severe pulmonary edema. Immunostaining using a neutrophil-specific antibody demonstrated more neutrophil infiltration in LPS-treated VDR-null lung compared with WT lung (Figure 1D). Moreover, TUNEL staining revealed a marked increase in apoptosis in the lung from LPS-treated VDR KO mice (Figure 1, E and F), consistent with previous reports that endotoxin induces apoptosis of lung endothelial and epithelial cells (34, 35). There is no detectable apoptosis in WT and VDR KO lungs at baseline.

We further examined pulmonary vascular permeability and lung functions in these mice. Evans blue permeability assays showed a much more dramatic increase in vascular permeability in VDR KO mice compared with WT mice after LPS treatment (Figure 2A). VDR KO mice retained more fluid in the lung than WT mice at baseline and after LPS treatment (Figure 2B). LPS challenge also led to a greater increase in protein content and cell number in the BAL fluid in VDR KO mice than in WT mice (Figure 2, C and D), confirming that the VDR-null endothelial barrier is more permeable than the WT barrier in this setting. Moreover, LPS induced greater MPO activity in the lung of KO mice compared with WT mice (Figure 2 E), consistent with the immunostaining data showing more neutrophil infiltration in LPS-treated VDR-null lung (Figure 1D). Together these data demonstrated increased pulmonary vascular permeability in VDR KO mice following LPS challenge. Finally we measured the elastic resistance of the lung using a computer-controlled ventilator. VDR KO mice showed greater elastic resistance compared with WT mice both at baseline and after LPS treatment (Figure 2F), suggesting impaired respiratory functions in the KO mice. Further examination of the BAL showed significantly higher concentrations of proinflammatory cytokines IL-6 and TNFα in the BAL fluid obtained from LPS-treated KO mice compared with WT mice (Figure 3, A and B). Taken together these observations indicate that LPS causes more severe lung injury in VDR KO mice than in WT mice, which explains the higher mortality seen in the mutant mice. These results suggest that pathways regulated or mediated by the VDR inhibit the development of ALI.

VDR targets Ang-2-Tie-2 pathway in regulation of lung injury

Ang-2 plays a key role in ALI. Because $1,25(OH)_2D_3$ was reported to suppress Ang-2 expression in endothelial cells (36), we examined the Ang-2-Tie-2-MLCK pathway in the lung. LPS treatment for 24 hours induced pulmonary Ang-2 expression in both WT and KO mice, but Ang-2 induction was much more robust in KO mice, reflected at Ang-2 mRNA transcript levels in the lung (Figure 4A), at Ang-2 protein levels in the BAL fluid (Figure 4, B and C) as well as at Ang-2 protein levels in total lung lysates (Figure 4, D and F). Tie-2 was highly expressed in the lung as expected, with levels moderately reduced in KO mice at baseline and after LPS treatment (Figure 4, E and F). LPS induced MLC phosphorylation in the lung of both WT and KO mice, but the induction was more dramatic in the KO mice (Figure 4, D and F). These observations suggest that the increased lung injury seen in VDR KO mice is caused, at least in part, by increased MLC phosphorylation by MLCK, which is activated by excessive pulmonary Ang-2.

Vitamin D suppresses Ang-2 expression in pulmonary endothelial cells

We further used HPAE cells to study vitamin D regulation of the Ang-2 pathway. Human VDR mRNA transcript was detectable in these cells (Figure 5A), indicating that they express VDR. Ang-2 mRNA was highly induced by LPS within 3–6 hours in these cells (Figure 5B), and this induction was blocked by $1,25(OH)_2D_3$ treatment (Figure 5, C and D). Moreover, LPS also dramatically induced MLCK and MLC phosphorylation, and these inductions were also attenuated by $1,25(OH)_2D_3$ (Figure 5, E and F). Because LPS activates NF-κB, whereas $1,25(OH)_2D_3$ suppresses NF-κB activation (37), we asked whether $1,25(OH)_2D_3$ suppresses LPS induction of Ang-2 by targeting NF-κB. By in silico analysis we identified a putative κB site (5′-GGGCATTTCC-3′) within the first intron of human *ANG-2* gene. EMSAs showed that LPS induced nuclear protein binding to this κB probe, and the binding was blocked when the cells were

treated with $1,25(OH)_2D_3$ (Figure 5G). ChIP assays demonstrated that LPS induced p65 bindings to this κB site in HPAE cells, which was attenuated in the presence of $1,25(OH)_2D_3$ (Figure 5H). Together these data suggest that $1,25(OH)_2D_3$ blocks LPS-induced Ang-2 expression by targeting NF-κB.

Blockade of Ang-2 signaling ameliorates VDR-null lung injury

To confirm the role of the overproduced Ang-2 in the development of hyper severe lung injury in KO mice, we pretreated the mice with L1–10, an Ang-2 antagonist, for 2 weeks before LPS challenge. Compared with saline control, L1–10 pretreatment substantially attenuated pulmonary vascular leakiness and inflammation in KO mice, as demonstrated by reduction in Evans blue accumulation in the lung (Figure 6A), in BAL protein content (Figure 6B), and in lung MPO activity (Figure 6C). IL-6 levels in BAL fluid were also markedly decreased in KO mice after L1–10 pretreatment (Figure 6D). These results demonstrate that VDR signaling attenuates lung injury by targeting the Ang-2-Tie-MLCK pathway. The effect of L1–10 on WT mice, however, was less prominent, except for the reduction of BAL IL-6 levels. It is plausible that a higher dose of L1–10 is needed to substantially affect the course of ALI in WT mice.

The RAS is involved in VDR regulation of lung injury

Our previous studies demonstrated that $1,25(OH)_2D_3$ is a key negative regulator of the RAS and that VDR KO mice develop hyperreninemia with high circulating angiotensin II levels (38). Because angiotensin II is a mediator of lung injury, we examined renin and angiotensin II in the lung. Indeed, renin activity and angiotensin II levels in the BAL fluid were markedly induced in LPS-treated WT and KO mice; however, the elevation of renin activity and angiotensin II concentration were much more robust in KO mice compared with WT mice (Figure 7, A and B). To address whether the severe ALI seen in VDR KO mice was attributable to angiotensin II overproduction, we pretreated the mice with AT1 receptor antagonist losartan (in drinking water) for 2 weeks before LPS challenge. Compared with control (water), losartan pretreatment partially attenuated LPS-induced lung injury in KO mice, manifested by a reduction in Evans blue leakiness (Figure 7C), in cell number in the BAL fluid (Figure 7D) and in BAL protein concentration (Figure 7E). Therefore, these results suggest that VDR signaling protects the integrity of pulmonary vascular barrier by regulating the RAS as well.

Discussion

In this report we provide evidence that VDR-mediated $1,25(OH)_2D_3$ activity attenuates LPS-induced ALI. Our data suggest that VDR protects the integrity of the pulmonary vascular barrier by inhibiting the Ang-2-Tie-2 pathway as well as the RAS cascade. These actions result in suppression of MLCK and MLC phosphorylation, key molecular events that lead to increased vascular permeability, as well as blockade of cell apoptosis in the lung, which together contribute to lung protection (Figure 8).

ALI is a feature of LPS-induced sepsis. In LPS-induced ALI models, there are several routes for LPS delivery. Whereas intratracheal instillation of LPS causes lung injury from the alveolar epithelial side, iv or ip delivery of LPS directly damages capillary endothelial cells (39). In this study we used a LPS-induced sepsis model to study the role of VDR in ALI. By comparing the lung phenotype of LPS-treated WT and VDR KO mice, we found that KO mice developed much more severe lung injury after LPS challenge, which most likely accounts for their high death rate. Histologically KO mice showed increased pulmonary

edema, neutrophil infiltration, and apoptosis in the lung. We used several methods to assess the vascular damage of the lung, and the data confirmed that LPS caused more vascular damage in VDR KO mice leading to increased pulmonary vascular permeability, which eventually impaired the lung function. These results strongly suggest that VDR signaling is protective in the lung, because this pulmonary protection is lost with VDR deletion.

Our data suggest that an excessive induction of Ang-2 and angiotensin II in the lung accounts for the excessive lung injury seen in VDR KO mice. That Ang-2-Tie-2 signaling pathway plays a key role in ALI has been well established (11, 12). The induction of Ang-2 by LPS was much more robust in the lung of VDR KO mice relative to WT mice, reflected by mRNA and protein levels of Ang-2, including the secreted form in the BAL. MLC phosphorylation, a downstream molecular event of Ang-2-Tie-2 signaling leading to lung damage, was also excessively induced in the lung of KO mice. Moreover, we confirmed that $1,25(OH)_2D_3$ blocked LPS induction of Ang-2 as well as MLCK and MLC phosphorylation in HPAE cell cultures. Importantly, pretreatment of VDR KO mice with Ang-2 antagonist L1–10 markedly attenuated the severity of LPS-induced lung injury. Together these several lines of evidence support the conclusion that vitamin D-VDR protects the pulmonary vascular barrier, at least in part, by targeting the Ang-2-Tie-2-MLCK pathway, namely by suppressing Ang-2 expression (Figure 8). Meanwhile, we also detected excessive induction of renin activity and angiotensin II in the lung of LPS-treated KO mice. Because angiotensin II is another mediator of ALI (17, 18), this observation suggests an involvement of the RAS in sepsis-induced ALI in the absence of VDR protection. Indeed, when VDR KO mice were pretreated with losartan to block angiotensin II signaling, the severity of lung injury induced by LPS was attenuated. Therefore, VDR signaling appears to regulate both the Ang-2 and the RAS pathways in pulmonary protection. It is known that LPS induces lung endothelial and epithelial cell apoptosis (34, 35, 40), and pharmacologic blockade of angiotensin II type 1 receptor reduces lung cell apoptosis in animals (17, 41). Indeed, angiotensin II is known to activate p38 MAPK to induce apoptosis (42). Therefore, we speculate that high angiotensin II levels might be responsible for the marked increase in apoptosis detected in the lung of VDR KO mice (Figure 8). More investigations are needed to confirm this speculation.

What are the molecular mechanisms that account for VDR regulation of the Ang-2 and RAS pathways? Our in vitro studies in HPAE cells suggest that vitamin D down-regulates LPS-induced Ang-2 expression by targeting NF-κB. NF-κB is a key downstream mediator of the LPS-TLR4 signaling pathway, and vitamin D blockade of NF-κB activation has been well documented by us and other investigators (37, 43). Our recent studies showed that the underlying mechanism is that VDR blocks NF-κB activation by physically interacting with IκB kinase β protein, which disrupts IκB kinase complex formation leading to stabilization of IκBα (44). Here we identified a κB site in the first intron of human *ANG-2* gene that is bound by NF-κB p65, and we also demonstrated that this binding could be blocked by $1,25(OH)_2D_3$ in HPAE cells. These data support that NF-κB mediates the down-regulation of Ang-2 by the $1,25(OH)_2D_3$-VDR signaling (Figure 8). On the other hand, high renin and angiotensin II levels also contribute to lung injury in VDR KO mice. Angiotensin II overproduction in VDR KO mice was well documented previously as a result of renin overexpression (38). It is well established that $1,25(OH)_2D_3$ is a negative endocrine regulator of renin gene expression. VDR deletion results in renin up-regulation in the kidney, leading to hyperreninemia, serum angiotensin II elevation, and development of hypertension in VDR KO mice (38). We have already elucidated the molecular mechanisms whereby $1,25(OH)_2D_3$ down-regulates

renin gene expression and angiotensinogen gene expression. $1,25(OH)_2D_3$-VDR inhibits renin gene expression by blocking the cAMP-protein kinase A pathway that is essential to maintain renin gene expression (33). $1,25(OH)_2D_3$-VDR attenuates angiotensinogen expression by blocking NF-κB activation (45). Therefore, the mechanistic insights for vitamin D to regulate the Ang-2 and RAS pathways in pulmonary protection have been defined (Figure 8).

This study contributes to our understanding of VDR's role in lung biology. With regard to the relationship between VDR and the respiratory system, there have been epidemiologic data that suggested a link between vitamin D deficiency and asthma (22–24). Some VDR polymorphisms were associated with susceptibility of childhood and adult asthma (46, 47), whereas some VDR polymorphisms were thought to have a possible protective effect for unaffected children relative to children with asthma (48). There is also evidence for beneficial effects of vitamin D supplementation on asthma development (49) and for $1,25(OH)_2D_3$ modulation of chemokine expression in human airway smooth muscle cells (50). $1,25(OH)_2D_3$ has been reported to regulate genes in bronchial smooth muscle cells that are involved in autocrine, contractility, and remodeling processes (36). The role of VDR in lung biology, however, is not without controversies. For example, it was reported that VDR-null mice failed to develop experimental allergic asthma (51), but the failure to develop asthma was not seen in the vitamin D-deficient state (52). In contrast to our data, a recent study reported that vitamin D deficiency had little effects on LPS-induced lung injury in mice (53). The reason behind this discrepancy is unclear. It could be due to differences in LPS delivery routes (ip vs intratracheal) or in LPS doses used in these studies. Or it might be possible that the pulmonary protective effect of VDR is ligand independent. In any case, given the discrepancies between vitamin D deficiency and VDR deficiency and the scarcity of knowledge about pulmonary VDR function, more investigations are needed to fully elucidate the role of vitamin D-VDR signaling in the respiratory system.

Finally, potential protective effects of immune VDR signaling against ALI also need to be considered. In the LPS-induced sepsis model, LPS, in addition to directly damaging capillary endothelial cells, concomitantly induces a robust inflammatory response. Lung infiltration of immune cells, particularly neutrophils and macrophages, and proinflammatory cytokines produced by inflamed immune cells, also contributes to lung injury. In this regard, we recently demonstrated that macrophages with VDR deletion are hyperresponsive to LPS in terms of inflammatory reaction because of impaired negative feedback regulation (37). Therefore, the hyperactive VDR-null immune cells may contribute to the severe lung injury phenotype seen in VDR KO mice, implicating an inhibitory role of immune VDR actions in ALI. Certainly this issue warrants further investigations as well.

Acknowledgments

We thank Amgen Corp for providing L1–10 for this study.

This work was supported by American Heart Association Scientist Development Grant 10SDG4280066 (to J.K.), National Institutes of Health grants R01HL085793; (to Y.C.L.), R01DK092143;, and R01DK84974 (to R.T.), CTSA grant UL1 RR024999 from National Center for Research Resources, as well as by National Natural Science Foundation of China (Grants 30971401; and 81170065).

Author contributions: J.K. and Y.C.L. designed the research; J.K., X.Z., Y.S., and T.L. performed the study; X.Z. and Y.C. provided research reagents and technical assistance; J.K., X.Z., I.B., Q.Z., and R.T. assisted in data analysis and manuscript preparation; and Y.C.L. wrote the manuscript. Y.C.L. was responsible for overall research design, data analysis, and paper preparation.

Disclosure Summary: The authors declare no conflicts of interest.

Footnotes

Abbreviations:

ALI acute lung injury
Ang-2 angiopoietin-2
ARDS acute respiratory distress syndrome
BAL broncho-alveolar lavage
ChIP chromatin immunoprecipitation
HPAE human pulmonary artery endothelial
KO knockout
LPS lipopolysacchride
MLC myosin light chain
MLCK MLC kinase
NF-κB nuclear factor-{kappa]B
$1,25(OH)_2D_3$ 1,25-dihydroxyvitamin D_3
MPO myeloperoxidase
RAS renin-angiotensin system
TUNEL terminal deoxynucleotide transferase-mediated dUTP nick end labeling
VDR vitamin D receptor
WT wild type.

References

1. Beck-Schimmer B, Schimmer RC, Pasch T. The airway compartment: chambers of secrets. News Physiol Sci. 2004;19:129–132 [PubMed: 15143208]

2. Ware LB, Matthay MA. The acute respiratory distress syndrome. N Engl J Med. 2000;342(18):1334–1349 [PubMed: 10793167]

3. Garcia JG, Davis HW, Patterson CE. Regulation of endothelial cell gap formation and barrier dysfunction: role of myosin light chain phosphorylation. J Cell Physiol. 1995;163(3):510–522 [PubMed: 7775594]

4. Tinsley JH, Teasdale NR, Yuan SY. Myosin light chain phosphorylation and pulmonary endothelial cell hyperpermeability in burns. Am J Physiol Lung Cell Mol Physiol. 2004;286(4):L841–L847 [PubMed: 14672924]

5. Verin AD, Patterson CE, Day MA, Garcia JG. Regulation of endothelial cell gap formation and barrier function by myosin-associated phosphatase activities. Am J Physiol. 1995;269(1 Pt 1):L99–L108 [PubMed: 7631821]

6. Dudek SM, Garcia JG. Cytoskeletal regulation of pulmonary vascular permeability. J Appl Physiol. 2001;91(4):1487–1500 [PubMed: 11568129]

7. Wong AL, Haroon ZA, Werner S, Dewhirst MW, Greenberg CS, Peters KG. Tie2 expression and phosphorylation in angiogenic and quiescent adult tissues. Circ Res. 1997;81(4):567–574 [PubMed: 9314838]

8. Bhatt AJ, Pryhuber GS, Huyck H, Watkins RH, Metlay LA, Maniscalco WM. Disrupted pulmonary vasculature and decreased vascular endothelial growth factor, Flt-1, and TIE-2 in human infants dying with bronchopulmonary dysplasia. Am J Respir Crit Care Med. 2001;164(10 Pt 1):1971–1980 [PubMed: 11734454]

9. Thurston G, Rudge JS, Ioffe E, et al. Angiopoietin-1 protects the adult vasculature against plasma leakage. Nat Med. 2000;6(4):460–463 [PubMed: 10742156]

10. Mei SH, McCarter SD, Deng Y, Parker CH, Liles WC, Stewart DJ. Prevention of LPS-induced acute lung injury in mice by mesenchymal stem cells overexpressing angiopoietin 1. PLoS Med. 2007;4(9):e269. [PMCID: PMC1961632] [PubMed: 17803352]

11. Parikh SM, Mammoto T, Schultz A, et al. Excess circulating angiopoietin-2 may contribute to pulmonary vascular leak in sepsis in humans. PLoS Med. 2006;3(3):e46. [PMCID: PMC1334221] [PubMed: 16417407]

12. Orfanos SE, Kotanidou A, Glynos C, et al. Angiopoietin-2 is increased in severe sepsis: correlation with inflammatory mediators. Crit Care Med. 2007;35(1):199–206 [PubMed: 17110873]

13. Brindle NP, Saharinen P, Alitalo K. Signaling and functions of angiopoietin-1 in vascular protection. Circ Res. 2006;98(8):1014–1023 [PMCID: PMC2270395] [PubMed: 16645151]

14. Mofarrahi M, Nouh T, Qureshi S, Guillot L, Mayaki D, Hussain SN. Regulation of angiopoietin expression by bacterial lipopolysaccharide. Am J Physiol Lung Cell Mol Physiol. 2008;294(5):L955–L963 [PubMed: 18310225]

15. Eutamene H, Theodorou V, Schmidlin F, et al. LPS-induced lung inflammation is linked to increased epithelial permeability: role of MLCK. Eur Respir J. 2005;25(5):789–796 [PubMed: 15863634]

16. Imai Y, Kuba K, Rao S, et al. Angiotensin-converting enzyme 2 protects from severe acute lung failure. Nature. 2005;436(7047):112–116 [PMCID: PMC7094998] [PubMed: 16001071]

17. Liu L, Qiu HB, Yang Y, Wang L, Ding HM, Li HP. Losartan, an antagonist of AT1 receptor for angiotensin II, attenuates lipopolysaccharide-induced acute lung injury in rat. Arch Biochem Biophys. 2009;481(1):131–136 [PubMed: 18940180]

18. Wang F, Xia ZF, Chen XL, Jia YT, Wang YJ, Ma B. Angiotensin II type-1 receptor antagonist attenuates LPS-induced acute lung injury. Cytokine. 2009;48(3):246–253 [PubMed: 19748795]

19. Haussler MR, Whitfield GK, Haussler CA, et al. The nuclear vitamin D receptor: biological and molecular regulatory properties revealed. J Bone Miner Res. 1998;13(3):325–349 [PubMed: 9525333]

20. Haussler MR, Whitfield GK, Kaneko I, et al. Molecular mechanisms of vitamin D action. Calcif Tissue Int. 2013;92(2):77–98 [PubMed: 22782502]

21. Bouillon R, Carmeliet G, Verlinden L, et al. Vitamin D and human health: lessons from vitamin D receptor null mice. Endocr Rev. 2008;29(6):726–776 [PMCID: PMC2583388] [PubMed: 18694980]

22. Ginde AA, Mansbach JM, Camargo CA., Jr Vitamin D, respiratory infections, and asthma. Curr Allergy Asthma Rep. 2009;9(1):81–87 [PubMed: 19063829]

23. Litonjua AA, Weiss ST. Is vitamin D deficiency to blame for the asthma epidemic? J Allergy Clin Immunol. 2007;120(5):1031–1035 [PubMed: 17919705]

24. Grant WB. Hypothesis–ultraviolet-B irradiance and vitamin D reduce the risk of viral infections and thus their sequelae, including autoimmune diseases and some cancers. Photochem Photobiol. 2008;84(2):356–365 [PubMed: 18179620]

25. Li YC, Pirro AE, Amling M, et al. Targeted ablation of the vitamin D receptor: an animal model of vitamin D-dependent rickets type II with alopecia. Proc Natl Acad Sci USA. 1997;94(18):9831–9835 [PMCID: PMC23277] [PubMed: 9275211]

26. Li YC, Amling M, Pirro AE, et al. Normalization of mineral ion homeostasis by dietary means prevents hyperparathyroidism, rickets, and osteomalacia, but not alopecia in vitamin D receptor-ablated mice. Endocrinology. 1998;139(10):4391–4396 [PubMed: 9751523]

27. Peng X, Hassoun PM, Sammani S, et al. Protective effects of sphingosine 1-phosphate in murine endotoxin-induced inflammatory lung injury. Am J Respir Crit Care Med. 2004;169(11):1245–1251 [PubMed: 15020292]

28. Rojas M, Woods CR, Mora AL, Xu J, Brigham KL. Endotoxin-induced lung injury in mice: structural, functional, and biochemical responses. Am J Physiol Lung Cell Mol Physiol. 2005;288(2):L333–L341 [PubMed: 15475380]

29. Quintero PA, Knolle MD, Cala LF, Zhuang Y, Owen CA. Matrix metalloproteinase-8 inactivates macrophage inflammatory protein-1α to reduce acute lung inflammation and injury in mice. J Immunol. 2010;184(3):1575–1588 [PMCID: PMC2938777] [PubMed: 20042585]

30. Wang Y, Deb DK, Zhang Z, et al. Vitamin D receptor signaling in podocytes protects against diabetic nephropathy. J Am Soc Nephrol. 2012;23(12):1977–1986 [PMCID: PMC3507366] [PubMed: 23123403]

31. Zhang Z, Sun L, Wang Y, et al. Renoprotective role of the vitamin D receptor in diabetic nephropathy. Kidney Int. 2008;73(2):163–171 [PubMed: 17928826]

32. Li YC, Bolt MJ, Cao LP, Sitrin MD. Effects of vitamin D receptor inactivation on the expression of calbindins and calcium metabolism. Am J Physiol Endocrinol Metab. 2001;281:E558–E564 [PubMed: 11500311]

33. Yuan W, Pan W, Kong J, et al. 1,25-Dihydroxyvitamin D3 suppresses renin gene transcription by blocking the activity of the cyclic AMP response element in the renin gene promoter. J Biol Chem. 2007;282(41):29821–29830 [PubMed: 17690094]

34. Kawasaki M, Kuwano K, Hagimoto N, et al. Protection from lethal apoptosis in lipopolysaccharide-induced acute lung injury in mice by a caspase inhibitor. Am J Pathol. 2000;157(2):597–603 [PMCID: PMC1850133] [PubMed: 10934162]

35. Kitamura Y, Hashimoto S, Mizuta N, et al. Fas/FasL-dependent apoptosis of alveolar cells after lipopolysaccharide-induced lung injury in mice. Am J Respir Crit Care Med. 2001;163(3 Pt 1):762–769 [PubMed: 11254536]

36. Bossé Y, Maghni K, Hudson TJ. 1α,25-Dihydroxy-vitamin D3 stimulation of bronchial smooth muscle cells induces autocrine, contractility, and remodeling processes. Physiol Genomics. 2007;29(2):161–168 [PubMed: 17213369]

37. Chen Y, Liu W, Sun T, et al. 1,25-Dihydroxyvitamin D promotes negative feedback regulation of TLR signaling via targeting microRNA-155-SOCS1 in macrophages. J Immunol. 2013;190(7):3687–3695 [PMCID: PMC3608760] [PubMed: 23436936]

38. Li YC, Kong J, Wei M, Chen ZF, Liu SQ, Cao LP. 1,25-Dihydroxyvitamin D(3) is a negative endocrine regulator of the renin-angiotensin system. J Clin Invest. 2002;110(2):229–238 [PMCID: PMC151055] [PubMed: 12122115]

39. Matute-Bello G, Frevert CW, Martin TR. Animal models of acute lung injury. Am J Physiol Lung Cell Mol Physiol. 2008;295(3):L379–L399 [PMCID: PMC2536793] [PubMed: 18621912]

40. Wang HL, Akinci IO, Baker CM, et al. The intrinsic apoptotic pathway is required for lipopolysaccharide-induced lung endothelial cell death. J Immunol. 2007;179(3):1834–1841 [PubMed: 17641050]

41. Podowski M, Calvi C, Metzger S, et al. Angiotensin receptor blockade attenuates cigarette smoke-induced lung injury and rescues lung architecture in mice. J Clin Invest. 2012;122(1):229–240 [PMCID: PMC3248282] [PubMed: 22182843]

42. Tsiani E, Lekas P, Fantus IG, Dlugosz J, Whiteside C. High glucose-enhanced activation of mesangial cell p38 MAPK by ET-1, ANG II, and platelet-derived growth factor. Am J Physiol Endocrinol Metab. 2002;282(1):E161–E169 [PubMed: 11739097]

43. Zhang Z, Yuan W, Sun L, et al. 1,25-Dihydroxyvitamin D_3 targeting of NF-κB suppresses high glucose-induced MCP-1 expression in mesangial cells. Kidney Int. 2007;72(2):193–201 [PubMed: 17507908]

44. Chen Y, Zhang J, Ge X, Du J, Deb DK, Li YC. Vitamin D receptor inhibits nuclear factor κB activation by interacting with IκB kinase β protein. J Biol Chem. 2013;288(27):19450–19458 [PMCID: PMC3707648] [PubMed: 23671281]

45. Deb DK, Chen Y, Zhang Z, et al. 1,25-Dihydroxyvitamin D_3 suppresses high glucose-induced angiotensinogen expression in kidney cells by blocking the NF-κB pathway. Am J Physiol Renal Physiol. 2009;296(5):F1212–F1218 [PMCID: PMC2681355] [PubMed: 19193728]

46. Poon AH, Laprise C, Lemire M, et al. Association of vitamin D receptor genetic variants with susceptibility to asthma and atopy. Am J Respir Crit Care Med. 2004;170(9):967–973 [PubMed: 15282199]

47. Raby BA, Lazarus R, Silverman EK, et al. Association of vitamin D receptor gene polymorphisms with childhood and adult asthma. Am J Respir Crit Care Med. 2004;170(10):1057–1065 [PubMed: 15282200]

48. Wjst M. Variants in the vitamin D receptor gene and asthma. BMC Genet. 2005;6(1):2. [PMCID: PMC546000] [PubMed: 15651992]

49. Hyppönen E, Sovio U, Wjst M, et al. Infant vitamin D supplementation and allergic conditions in adulthood: northern Finland birth cohort 1966. Ann NY Acad Sci. 2004;1037:84–95 [PubMed: 15699498]

50. Banerjee A, Damera G, Bhandare R, et al. Vitamin D and glucocorticoids differentially modulate chemokine expression in human airway smooth muscle cells. Br J Pharmacol. 2008;155(1):84–92 [PMCID: PMC2440089] [PubMed: 18552877]

51. Wittke A, Weaver V, Mahon BD, August A, Cantorna MT. Vitamin D receptor-deficient mice fail to develop experimental allergic asthma. J Immunol. 2004;173(5):3432–3436 [PubMed: 15322208]

52. Wittke A, Chang A, Froicu M, et al. Vitamin D receptor expression by the lung micro-environment is required for maximal induction of lung inflammation. Arch Biochem Biophys. 2007;460(2):306–313 [PMCID: PMC1933487] [PubMed: 17224129]

53. Klaff LS, Gill SE, Wisse BE, et al. Lipopolysaccharide-induced lung injury is independent of serum vitamin D concentration. PLoS One. 2012;7(11):e49076. [PMCID: PMC3501517] [PubMed: 23185294]

Figures and Tables

Figure 1.

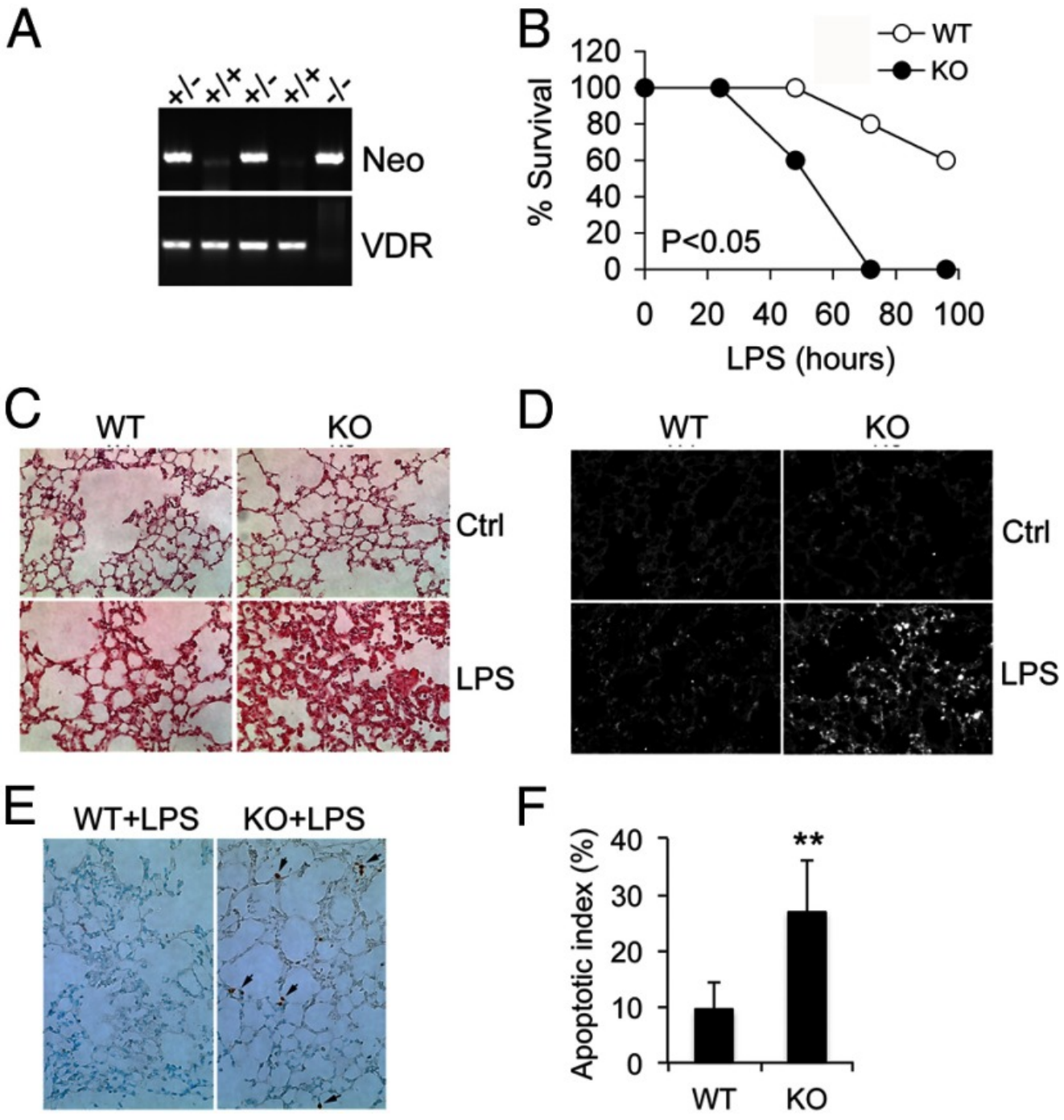

Open in a separate window

VDR inactivation leads to severe ALI after LPS challenge. WT and VDR KO mice were treated with saline or LPS (20 mg/kg, ip injection). A, Mouse genotyping. PCR product patterns indicate WT (+/+), heterozygote (+/−), and VDR KO (−/−) genotypes. B, Mouse survival curves after LPS treatment. C, Hematoxylin and eosin staining of lung sections from control (Ctrl) and LPS-treated WT and KO mice. Note the greater thickening of the alveolar interstitial space in LPS-treated KO mice. D, Fluorescent immunostaining of lung sections from control and LPS-treated WT and KO mice with

neutrophil-specific monoclonal antibodies 7/4. E and F, TUNEL staining of lung sections from LPS-treated WT and KO mice (E) and semiquantitation of the data (F). Apoptotic index is defined as percent of TUNEL-positive microscopic fields in randomly chosen 50 fields in each mouse. Arrows indicate TUNEL-positive cells. **, $P < .01$ vs WT.

Figure 2.

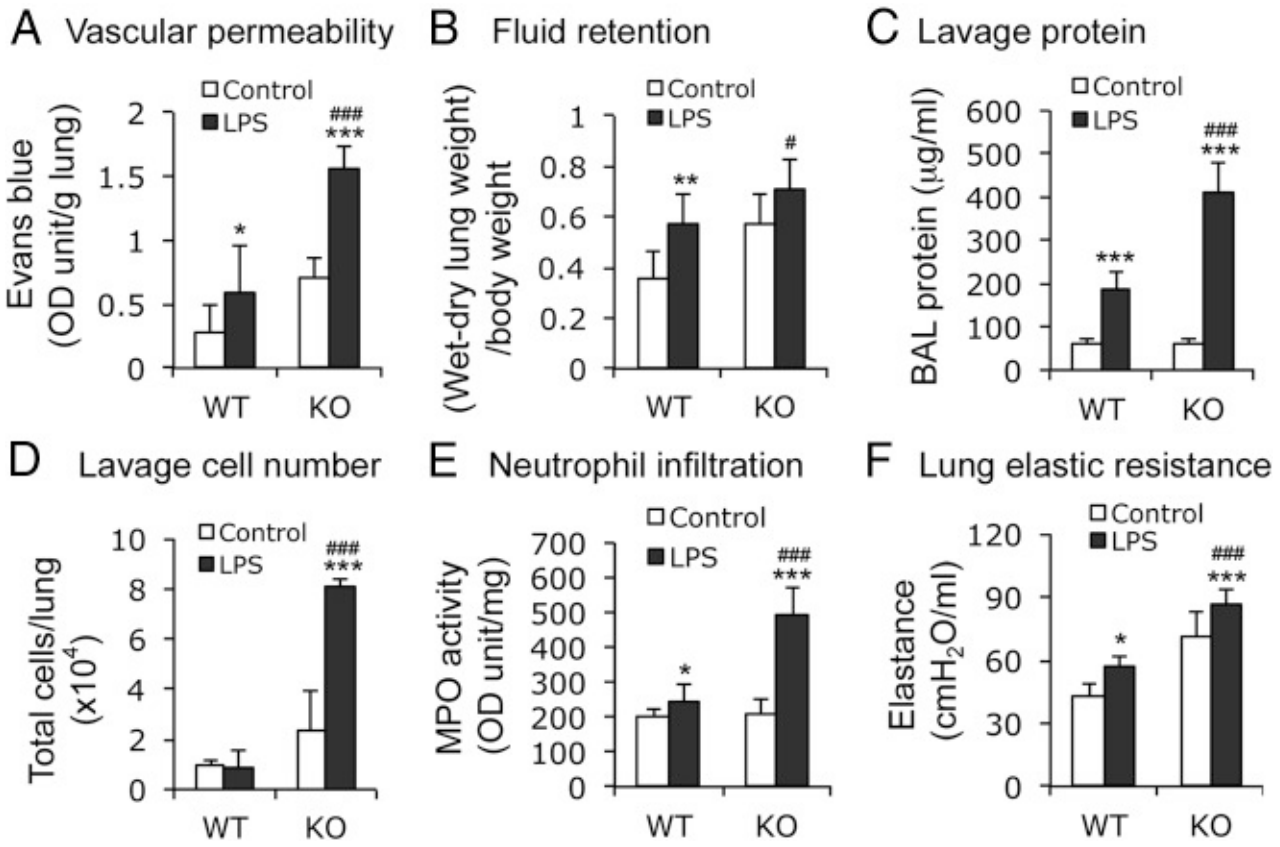

VDR deletion increases pulmonary vascular permeability and impairs lung function. WT and VDR KO mice were treated with saline (control) or LPS (20 mg/kg) via ip injection, and lung analyses were performed after 24 hours. A, Evans blue permeability assays. B, The difference of wet and dry weight of the lung (fluid retention) normalized to body weight. C, Protein concentration in the BAL. D, Cell number in BAL fluid. E, MPO activity in lung lysates. F, Lung elastic resistance. *, $P < .05$; **, $P < .01$; ***, $P < .001$ vs corresponding control of the same genotype; #, $P < .05$; ###, $P < .001$ vs LPS-treated WT; n = 5–6 in each genotype.

Figure 3.

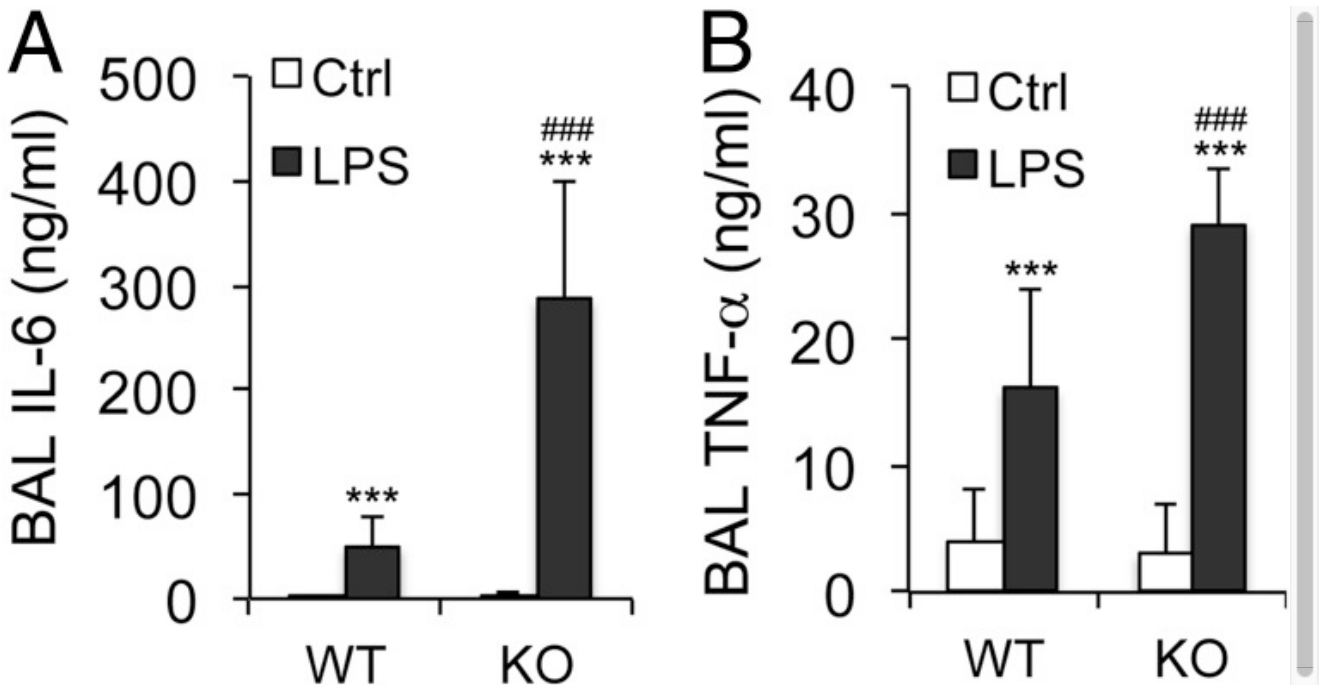

Open in a separate window

Proinflammatory cytokine levels in BAL fluids. WT and VDR KO mice were treated with saline (control [Ctrl]) or LPS, and levels of IL-6 (A) and TNFα (B) in BAL fluid were quantified by ELISA. ***, $P < .001$ vs corresponding control of the same genotype; ###, $P < .001$ vs LPS-treated WT; n = 5–6 in each genotype.

Figure 4.

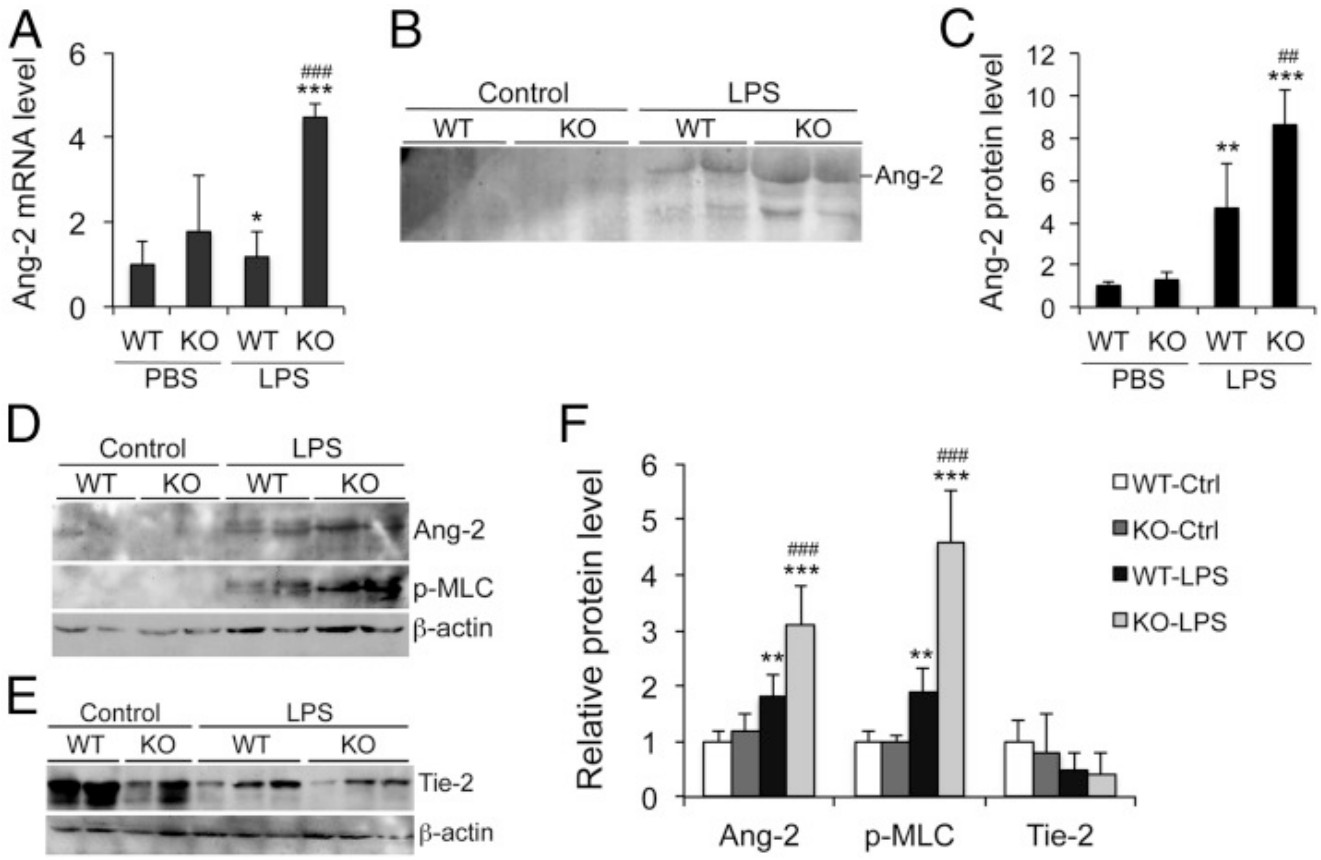

Open in a separate window

VDR signaling attenuates LPS-induced ALI by targeting the Ang-2-Tie-2-MLCK pathway. WT and VDR KO mice were treated with saline (control [Ctrl] or PBS) or LPS (20 mg/kg) by ip injection, and lung analyses were performed at 24 hours. A, Ang-2 mRNA levels quantified by real time RT-PCR; *, $P < .05$; ***, $P < .001$ vs corresponding control of the same genotype; ###, $P < .001$ vs LPS-treated WT; n = 4. B and C, Western blot analysis (B) and densitometric quantitation (C) of Ang-2 protein levels in BAL; **, $P < .01$; ***, $P < .001$ vs corresponding control of the same genotype; ###, $P < .001$ vs LPS-treated WT. D, Western blot analysis of Ang-2 protein and phosphorylated MLC (p-MLC) levels in total lung lysates. E, Western blot analysis of Tie-2 levels in total lung lysates. F, Densitometric quantitation of these Western blot data. **, $P < .01$; ***, $P < .001$ vs corresponding control of the same genotype; ###, $P < .001$ vs LPS-treated WT.

Figure 5.

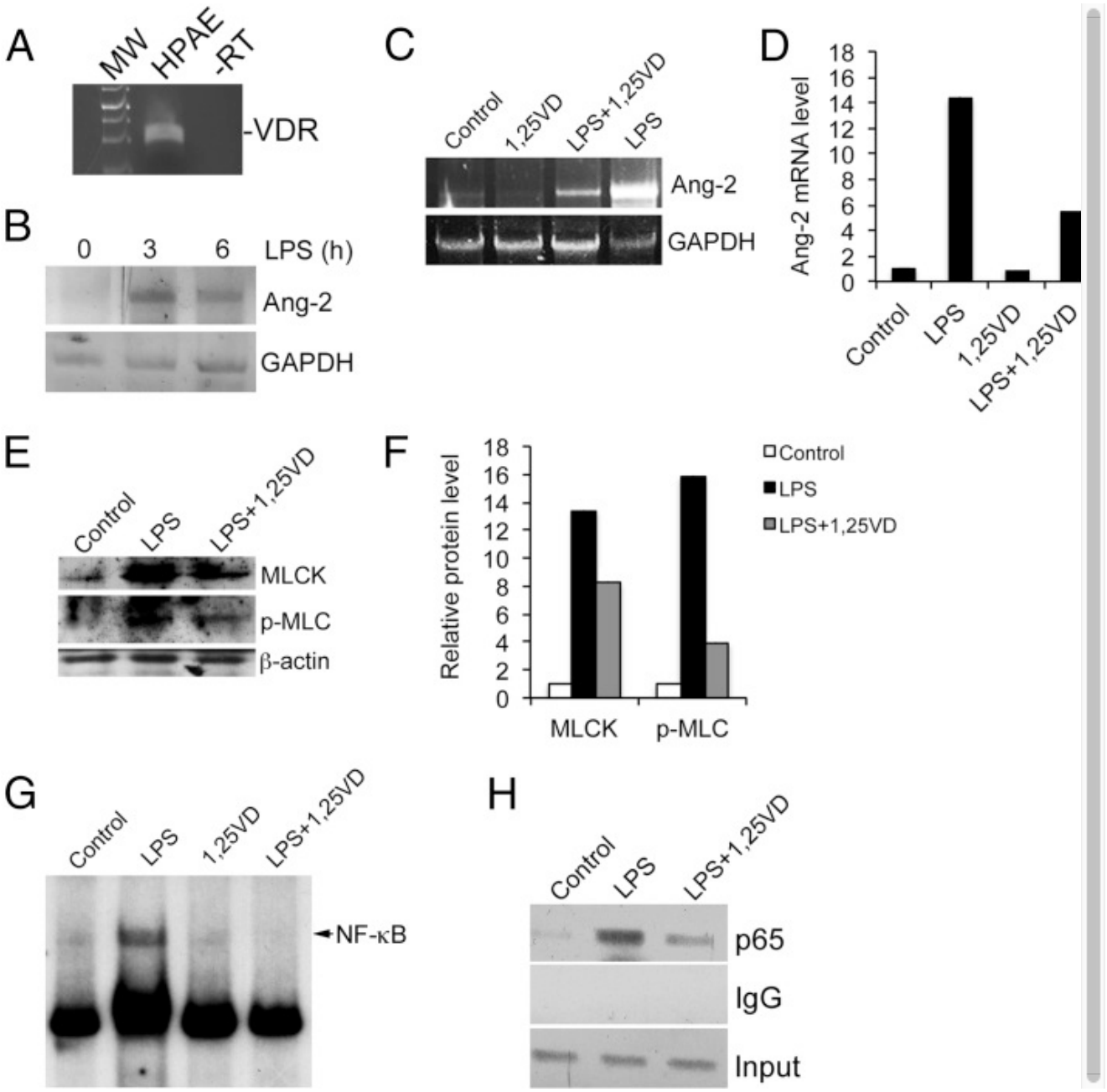

Open in a separate window

$1,25(OH)_2D_3$ down-regulates Ang-2 by targeting NF-κB activation in HPAE cells. A, RT-PCR detection of human VDR mRNA transcript in HPAE cells. −RT, minus reverse transcriptase control. B, HPAE cells were treated by LPS for 3 and 6 hours, and Ang-2 mRNA induction was measured by RT-PCR. C and D, HPAE cells were treated with LPS in the presence or absence of $1,25(OH)_2D_3$ (20 nM). Ang-2 mRNA was assessed by RT-PCR at 24 hours (C) and semiquantified by densitometry (D). E and F, HPAE cells were treated with LPS in the presence or absence of $1,25(OH)_2D_3$. MLCK and phosphorylated MLC levels were assessed by Western blotting after 24 hours (E) and semiquantified by densitometry (F). G, EMSA. HPAE cells were treated with LPS in the presence or absence of $1,25(OH)_2D_3$ for 24 hours. Nuclear extracts were prepared for EMSA using ^{32}P-labeled putative κB probe within the first intron of human *ANG-2* gene. H, ChIP assay. HPAE cells were treated with LPS in the presence or absence of $1,25(OH)_2D_3$ for 6 hours. ChIP assays were

performed using anti-p65 antibodies or nonimmune IgG. PCR amplification was performed using primers flanking the putative κB site within the first intron of human *ANG-2* gene. GAPDH, glyceraldehyde-3-phosphate dehydrogenase; MW, molecular weight; −RT, minus reverse transcriptase; 1,25VD, $1,25(OH)_2D_3$; p-MLC, phosphorylated MLC.

Figure 6.

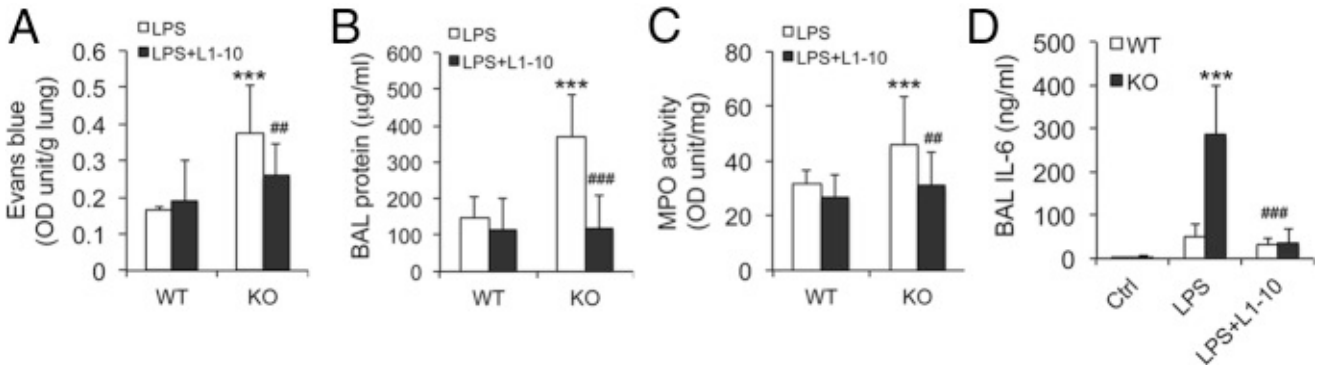

Blockade of Ang-2 signaling ameliorates lung injury in VDR-null mice. WT and KO mice were pretreated with saline or L1–10 for 2 weeks followed by LPS challenge. Lung damage analyses were performed 24 hours after LPS treatment. A, Evans blue permeability assay. B, Total protein concentrations in the BAL. C, MPO activity in total lung lysates. D, IL-6 levels in the BAL fluid. ***, $P < .001$ vs LPS-treated WT; ##, $P < .01$; ###, $P < .001$ vs LPS-treated KO; n = 5–6 in each genotype. Ctrl, control.

Figure 7.

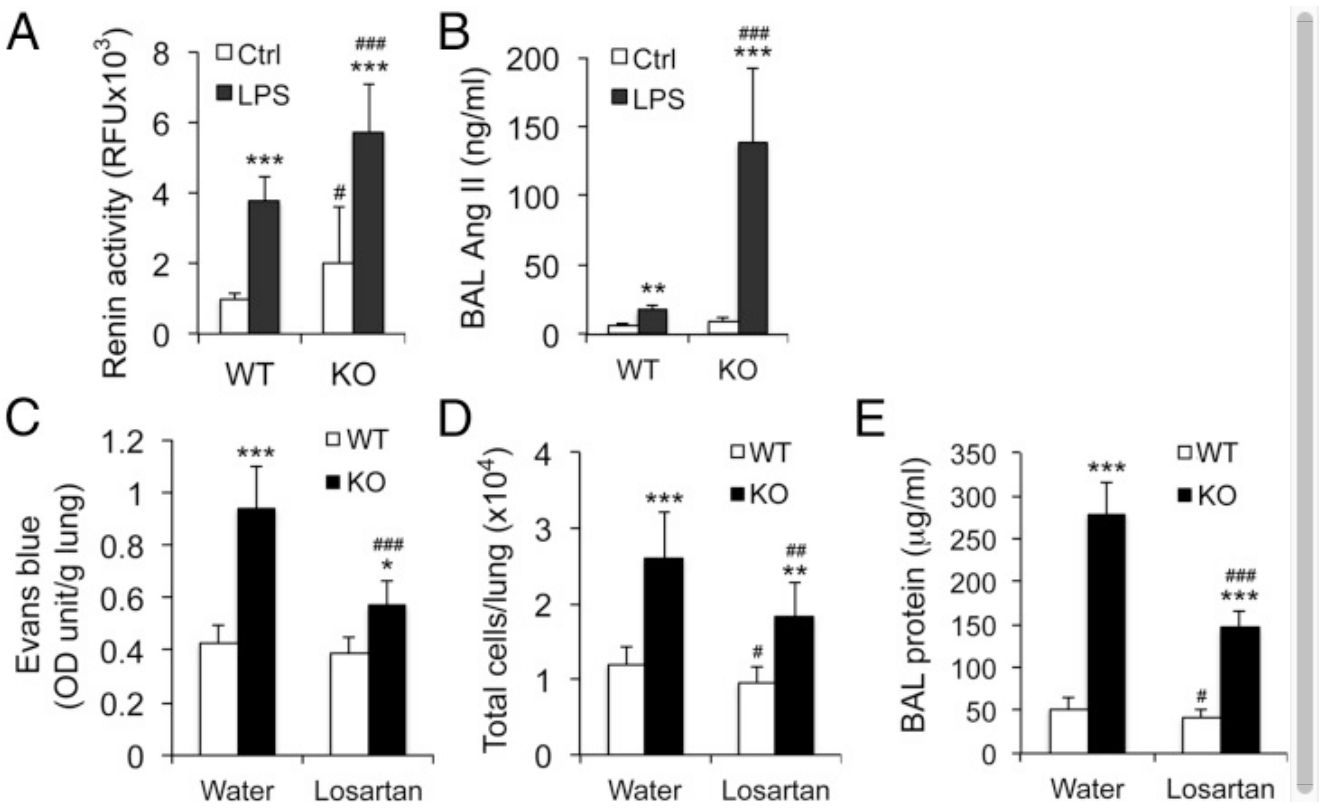

VDR signaling attenuates LPS-induced ALI by targeting the RAS. A and B, WT and KO mice were treated with saline (Ctrl) or LPS (20 mg/kg). Renin activity (A) and angiotensin II levels (B) in the BAL fluid were measured at 24 hours. **, $P < .01$; ***, $P < .001$ vs control of the same phenotype; #, $P < .05$; ##, $P < .001$ vs corresponding WT of the same treatment; n = 5–6 each genotype. C–E, WT and KO mice were fed regular water or losartan-containing water for 2 weeks followed by LPS challenge. Lung damage analyses were performed 24 hours after LPS treatment. C, Evans blue permeability assay. D, Total cell number in the BAL fluid. E, Total protein concentration in the BAL fluid. *, $P < .05$; **, $P < .01$; ***, $P < .001$ vs WT of the same treatment; ##, $P < .01$; ###, $P < .001$ vs KO fed regular water; n = 5–6 in each genotype.

Figure 8.

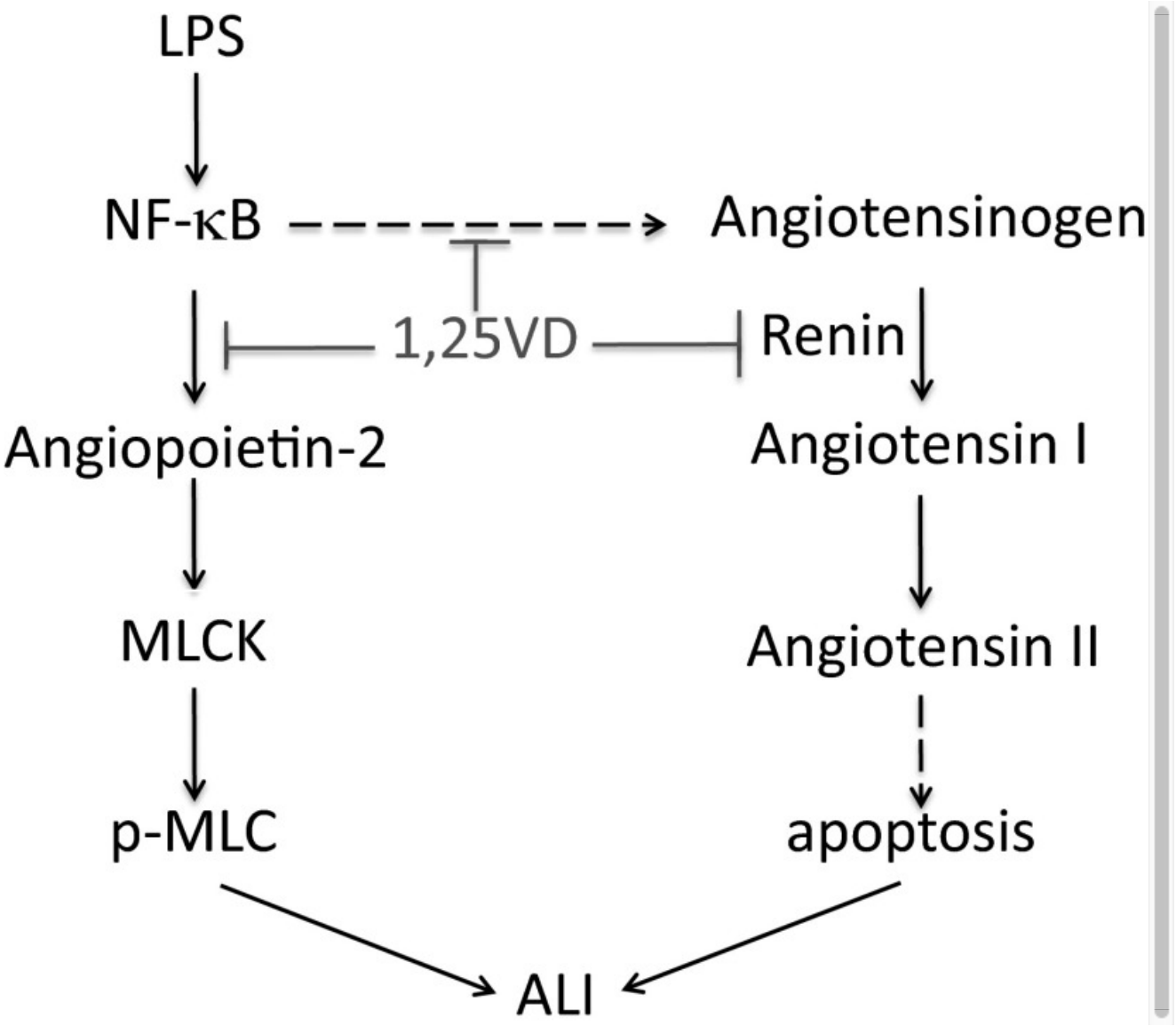

Open in a separate window

Proposed mechanism whereby 1,25$(OH)_2D_3$-VDR signaling inhibits the Ang-2-Tie-2-MLCK pathway and the RAS cascade to attenuate LPS-induced ALI. Dashed line indicates speculation. p-MLC, phosphorylated MLC; 1,25VD, 1,25$(OH)_2D_3$.